Inhibition of cell survival and invasion by Tanshinone IIA via FTH1: A key therapeutic target and biomarker in head and neck squamous cell carcinoma

WEI MAO*, JIAN DING*, YU LI, RUOFEI HUANG and BAOXIN WANG

Division of Otolaryngology-Head and Neck Surgery, Shanghai General Hospital of Jiaotong University, Key Laboratory of Head and Neck, Shanghai 200080, P.R. China

Received February 9, 2022; Accepted May 23, 2022

DOI: 10.3892/etm.2022.11449

Abstract. Head and neck squamous cell carcinoma (HNSCC) is a worldwide public health problem; its incidence is increasing and it is now the sixth most common cancer type worldwide. As indicated by existing studies, ferroptosis contributes to HNSCC progression and Tanshinone IIA (TanIIA) may exert therapeutic effects via affecting ferroptosis. However, the underlying mechanisms have remained to be clarified. Therefore, the main aim of the present study was to screen and investigate the key genes in regulating ferroptosis of the human hypopharynx squamous carcinoma cell line FaDu and further elucidate the mechanism of action of TanIIA. A list of ferroptosis-related genes was obtained from the FerrDb database. RNA-sequencing expression (level 3) profiles and corresponding clinical information (cases, n=502; normal controls, n=44) were downloaded from The Cancer Genome Atlas dataset for HNSCC (https://portal.gdc.com). The limma package in R software was used to study the differentially expressed mRNAs. Adjusted P<0.05 and Log2(fold change) >1 or <-1 were defined as the threshold for the differential expression of mRNAs. The ClusterProfiler package (version 3.18.0) in R was employed to analyze the Gene Ontology functional terms associated with potential targets and perform a Kyoto Encyclopedia of Genes and Genomes pathway analysis. The R package ggplot2 was used to draw the boxplot and the pheatmap package was used to draw the heatmap. The DEG-related protein-protein interaction network was built with the Search Tool for the Retrieval of Interacting Genes and proteins database and then the visualization was performed using Cytoscape. Ferritin heavy chain 1 (FTH1), transferrin (TF) and TF receptor were screened out using a Wayne diagram, which was drawn by the Venn Diagram package in R. Kaplan-Meier survival analysis and the log-rank test were used to compare differences in survival between the groups. The receiver operating characteristic (v 0.4) (ROC) curve analysis was used to compare the predictive accuracy of mRNAs. FTH1 was screened out and the expression results were verified using The Human Protein Atlas data. Immunohistochemistry and immunofluorescence were used to localize FTH1 expression in FaDu cells. Furthermore, Cell Counting Kit-8 and Transwell assays were used to detect the cell survival and invasion ability, respectively. Furthermore, western blot analysis was performed to analyze protein expression. The results of the present study indicated that three validated ferroptosis marker genes were differentially expressed in HNSCC, among which FTH1 was significantly associated with poorer survival. TanIIA was demonstrated to significantly affect FaDu cell survival and invasiveness and markedly attenuate FTH1 expression. To conclude, the ferroptosis gene FTH1 is highly expressed in HNSCC and TanIIA significantly inhibited HNSCC, partially by suppressing FTH1.

Correspondence to: Dr Ruofei Huang or Dr Baoxin Wang, Division of Otolaryngology-Head and Neck Surgery, Shanghai General Hospital of Jiaotong University, Key Laboratory of Head and Neck, 86 Wujin Road, Shanghai 200080, P.R. China
E-mail: hrf321@163.com
E-mail: Wbxshgh@163.com

*Contributed equally

Abbreviations: HNSCC, head and neck squamous cell carcinoma; TanIIA, Tanshinone IIA; DEG, differentially expressed gene; FTH1, ferritin heavy chain 1; TF, transferrin; TFR1, TF receptor protein 1; PPI, protein-protein interaction; CCK-8, Cell Counting Kit-8; DAPI, 4',6-diamidino-2-phenylindole; DMEM, Dulbecco's modified Eagle's medium; FBS, fetal bovine serum; IF, immunofluorescence; IHC, immunohistochemistry

Key words: head and neck squamous cell carcinoma, invasion, cell survival, ferritin heavy chain 1, ferroptosis, Tanshinone IIA

Introduction

Head and neck squamous cell carcinoma (HNSCC) is one of the most lethal malignancies with >800,000 new-onset cases reported per year. Mortality rates are increased with the stage of the disease and rates >50% have been identified in critically ill patients (1). HNSCC originates from epithelial cells of the upper respiratory tract and esophageal mucosa; of note, HNSCC exhibits high heterogeneity due to the complex anatomy and genetic variations in that area. Over the past few years, research on the correlation between ferroptosis and tumors has become a major research hotspot. Several studies

confirmed that the expression levels of ferroptosis proteins exhibited a wide variation in HNSCC, thereby significantly regulating cell proliferation (2) and epithelial-mesenchymal transformation (3) and even affecting cisplatin resistance (4). However, systematic studies focusing on ferroptosis and HNSCC have been continuously lacking thus far and research on novel precision therapy targets remains in its infancy.

Over the past decade, research on the significance of ferroptosis in cancer has gained momentum. Ferroptosis is another type of programmed necrotic cell death involving iron-dependent lipid peroxidation and oxidative stress is thought to be a principal cause of ferroptosis (5). Due to cancer cells' high iron levels and their increased sensitivity to ferroptosis induction, ferroptosis has been proposed to be promising for cancer therapeutics. A growing number of studies indicated that for numerous types of solid tumor, positive treatment effects were achieved by targeting ferroptosis-related genes.

Besides ferroptosis agonists and inhibitors, multiple drugs and Traditional Chinese Medicine (TCM) monomers were confirmed to effectively affect the level of ferroptosis and exert antitumor effects. Kong *et al* (6) proved that baicalin exerted its anticancer activity via ferritin heavy chain 1 (FTH1) in both 5637 and KU19-19 cells. Zhu *et al* (7) proposed that artemisinin and its derivatives may be used in the future as cancer therapies with broader applications due to their induction of ferroptosis. Tanshinone IIA (TanIIA) has long been confirmed to have a pivotal role in HNSCC treatment. Studies in other organs indicate that TanIIA exerts a significant impact on ferroptosis. For example, it has been proved that Tan IIA induced ferroptosis in BGC-823 and NCI-H87 gastric cancer cells via upregulating p53 expression and downregulating xCT expression in gastric cancer (8). However, the association between TanIIA and ferroptosis in HNSCC has remained elusive.

TanIIA, a pharmacologically active component isolated from the rhizome of the Chinese herb *Salvia miltiorrhiza* Bunge (Danshen), has been reported to possess pleiotropic effects, such as anti-inflammatory effects, antioxidant and anti-atherogenic effects. Recent studies have suggested that TanIIA exhibits highly potent antitumor activity by inducing apoptosis and triggering autophagy in tumor cells (9). A previous study by our group confirmed TanIIA has a significant effect to promote FaDu cell apoptosis by causing cell cycle arrest at the S phase, which resulted in observably higher apoptotic cell fractions and downregulation of survivin protein expression (10). In addition, TanIIA was confirmed to exert its protective effect on endothelial cells by inhibiting ferroptosis via activation of NRF2 (11). However, the exact target and mechanisms by which TanIIA regulates ferroptosis remain to be elucidated.

In the present study, data acquired from FerrDb were mined to comprehensively analyze the correlations between ferroptosis marker genes and HNSCC. Cell survival, invasion and expression status were evaluated after treatment with TanIIA, with the goal of uncovering the function of TanIIA.

Materials and methods

Data sources. The RNA-sequencing expression (level 3) profiles and corresponding clinical information for HNSCC were downloaded from The Cancer Genome Atlas (TCGA) dataset (portal.gdc.com), including 502 tumor samples and 44 normal controls. Ferroptosis-related genes were acquired from the FerrDb database [Zhou and Bao (12), 2020] which includes 125 ferroptosis marker genes, of which 9 genes have been verified.

Differentially expressed gene (DEG) analysis. The limma package in R (version 3.4.2; http://www.bioconductor.org/packages/release/bioc/html/limma.html) was used to analyze the differentially expressed mRNAs among samples. 'Adjusted P<0.05 and Log2 (Fold Change) >1 or Log2(Fold Change) <-1' were defined as the threshold for the differential expression of mRNAs. Spearman's correlation analysis was used to describe the correlation between the 9 marker genes. P<0.05 was considered to indicate statistical significance (Table SI). The DEG-related protein-protein interaction (PPI) network was established using the Search Tool for the Retrieval of Interacting Genes and proteins (STRING) database (string-db.org/) (13) (Table SII), followed by visualization using Cytoscape software (version 3.8.2; manual.cytoscape.org) (14).

To further confirm the underlying function of potential targets, the data were analyzed by functional enrichment. To better understand the role of these mRNAs in carcinogenesis, the ClusterProfiler package (version: 3.18.0) in R was employed to analyze the Gene Ontology function of potential targets and the Kyoto Encyclopedia of Genes and Genomes pathway. The R software ggplot2 package was used to draw the boxplot, while the R software pheatmap package was used to draw the heatmap.

Validated ferroptosis marker genes and HNSCC correlation analysis. The multi-gene correlation pheatmap was displayed by the R software package. Spearman's correlation analysis was used to determine the correlation between the 9 validated ferroptosis markers. A Venn diagram analysis was carried out between genes encoding ferroptosis markers and validated markers that are associated with DEGs using the Interacti-Venn website (interactivenn.net/; Table SIII). By the above means, FTH1, transferrin (TF) and TF receptor (TFRC) were screened out. The Human Protein Atlas (http://www.proteinatlas.org) was used to validate FTH1 expression in the alimentary system (which includes the larynx and hypopharynx).

The expression distributions of FTH1, TFRC and TF genes in tumor tissues and normal tissues were downloaded from the TCGA dataset. The current-release (V8) GTEx datasets were obtained from the GTEx data portal (https://www.gtexportal.org/home/datasets) website. Data were analyzed using R software v4.0.3 (R Foundation for Statistical Computing). P<0.05 was considered to indicate statistical significance.

Analyses of prognosis. Correlations between the expression levels of FTH1, TFRC and TF genes and HNSCC overall survival were separately analyzed through the Kaplan-Meier method and the log-rank test. Time-receiver operating characteristic (ROC; v 0.4) (15) analysis was used to compare the predictive accuracy of mRNA. All the analytic methods and R packages were implemented by R (foundation for statistical

computing 2020) version 4.0.3. Furthermore, images of protein immunohistochemistry (IHC) stains for FTH1, TFRC and TF in tumor tissues were obtained from the Human Protein Atlas (16).

Cell acquisition. FaDu and human hypopharyngeal cell lines were purchased from Procell Life Science & Technology Co., Ltd. The obtained cells were cultured and passaged as primary cells and then cultured in Dulbecco's modified Eagle's medium (DMEM; Gibco; Thermo Fisher Scientific, Inc.) containing 10% fetal bovine serum (FBS; Gibco; Thermo Fisher Scientific, Inc.) and 1% double antibody (penicillin-streptomycin mixture) (MilliporeSigma) in an incubator with 5% CO_2 at 37˚C. The cells were subcultured to the third passage.

IHC method. FTH1 expression was visualized using the IHC method. FaDu cells were seeded on to cover slips at $5x10^4$/ml density and then fixed in 4% paraformaldehyde (Beyotime Institute of Biotechnology) for 15 min at 37˚C, permeabilized using 0.1% Triton X-100 (Beyotime Institute of Biotechnology) for 20 min blocked using 5% bovine serum albumin (MilliporeSigma) for 1 h at 37˚C Heat-mediated antigen retrieval was performed with Tris/EDTA buffer (Gibco; Thermo Fisher Scientific, Inc.). A total of 100 μl reaction enhancer was added to the samples and incubated for 20 min at 37˚C before IHC staining (cat. no. PV-6000; Zhongshanjinqiao). The samples were then incubated with HRP-labeled secondary antibody (cat. no. A18781; 1:1,000 dilution; Thermo Fisher Scientific, Inc.) for 30 min at 37˚C, after which the nuclei were counterstained with diaminobenzidine (1:1,000; Beyotime Institute of Biotechnology, Inc.) for 5-8 min. Following washing with tap water, samples were stained with hematoxylin (Beyotime Institute of Biotechnology, Inc.) for 20 sec, then dehydrated with different concentrations of ethanol and clarified using dimethyl benzene (MilliporeSigma) solution. Images were captured with an inverted phase-contrast microscope (CH30; Olympus Corp.). A total of 5 images were acquired from different fields of view of each slide and the staining of yellow particles was regarded as positive expression.

Immunofluorescence (IF) method. IF assays were conducted to determine the cellular location of FTH1 protein expression. The pre-treatment procedure was the same as that used for IHC. IF was performed with FTH1 (5 μg/ml; cat. no. ab65080; Abcam) antibody for 12 h at 4˚C in the dark, followed by incubation with DyLight 488 conjugated, goat anti-human IgG (cat. no. ab96907; 1:1,000; Abcam.). The nuclei were stained with 4',6-diamidino-2-phenylindole (DAPI; Beijing Solarbio Science & Technology, Co., Ltd.). A total of five fluorescence images were captured using a fluorescence microscope (Leica DMi8; Leica Microsystems GmbH) with different excitation wavelengths for the same field (dylight488 maximum emission is 518 nm; DAPI maximum emission is 454 nm).

Cell survival. A Cell Counting Kit-8 assay (CCK-8; MedChemExpress) (17) was adopted to detect cell survival. TanIIA (cat. no. HY-N0135; MedChemExpress) was dissolved with DMSO using ultrasonication, followed by treatment for 24, 48 and 72 h at individual concentrations of 0.25, 0.5 or 1.0 mg/l as the treatment group. Cells were grown in 96-well plates and cell survival was measured after 24 h following the manufacturer's protocol. CCK-8 stain and serum-free medium were mixed at a volume ratio of 1:10 and incubated in 5% CO_2 at 37˚C for 1 h. The absorbance at 450 nm wavelength (optical density value) was then measured with a microplate reader (Multiskan-MK3; Thermo Fisher Scientific, Inc.).

Tumor invasive ability. The tumor cell invasion capacity was analyzed using a Transwell chamber (8.0 μm pore size; Corning, Inc.). BD Matrigel (cat. no. 354248; BD Biosciences), which had been frozen in a -80˚C freezer, was kept at 4 degrees overnight for 24 h, after which 300 μl serum-free medium was added to 60 μl Matrigel® to prepare a mixed solution and the upper chambers were coated with it in 24-well plates. FaDu cells ($1x10^5$) were then seeded into five 96-well plates ($1x10^3$ cells/well), with five parallel wells for each cell group. Furthermore, 500 μl DMEM (Gibco; Thermo Fisher Scientific, Inc.) containing 10% FBS was added to the lower chamber. The cells were then incubated for 24 h at 37˚C in a 5% CO_2 incubator. Transwell chambers were removed and cells that had transgressed through the membrane to the lower side were washed 2 times with PBS and fixed with 5% glutaraldehyde (Beijing Solarbio Science & Technology, Co., Ltd.) at 4˚C. The attached cells were stained with crystal violet (0.5% crystal violet in 20% methanol) for 5-10 min and then washed two times with PBS. Images were acquired using an Axiovert 40 CFL inverted microscope (Zeiss AG) and invaded cells were counted and recorded. Five fields per slide were used in the analysis and each experiment was performed in triplicate.

Western-blot analysis. FaDu and normal mucosa cells were seeded in 6-well plates at $5x10^4$/ml density (8 ml) and incubated overnight in a 5% CO_2 incubator at 37˚C. Cells were first starved in serum-free medium for 48 h, then treated with complete medium with 10% FBS for 12 h and treated with TanIIA at 0.5 mg/l for another 12 h. Cells cultured in a drug-free medium were used as the control group. Total proteins were extracted using One Step Animal Tissue/Cell Active Protein Extraction buffer (RIPA; Thermo Fisher Scientific, Inc.) Protein concentration was determined via BCA assay (cat. no. 23227; Thermo Fisher Scientific, Inc.). Equal amounts of total protein (40 μg) were loaded in each protein lane. Samples were separated by 10% SDS-PAGE (Beijing Solarbio Science & Technology, Co., Ltd.) using a Bio-Rad Electrophoresis System (Bio-Rad Laboratories, Inc.). The proteins were transferred to a nitrocellulose membrane (cat. no. IFPL00010; Merck KGaA) for gel electrophoresis separation, followed by blocking with 5% skimmed milk (cat. no. 232100; BD Difco) for 1 h. Tris-buffered saline with Tween-20 (Beijing Solarbio Science & Technology, Co., Ltd.) was used to wash the membranes, and subsequently, they were incubated at 4˚C overnight with the following primary antibodies: FTH1 (1 μg/ml; 21 kDa; cat. no. ab65080; Abcam); GAPDH (1:500 dilution; 36 kDa; cat. no. ab8245; Abcam). Subsequently, membranes were incubated with a 1:10,000 dilution of HRP-labeled secondary antibody (cat. no. 7076s; Cell Signaling Technology, Inc.) at room temperature for 1 h. GAPDH was used as a normalization control. The membrane was visualized using the ChemiDoc™ MP Imaging System (Bio-Rad Laboratories, Inc.) and analysis was performed using Image Lab software (v4.0; Bio-Rad Laboratories, Inc.).

Statistical analysis. Statistical analyses were performed using SPSS version 21.0 (IBM Corporation) and GraphPad Prism 8 (GraphPad Software, Inc.). Each experiment was performed in triplicate and the mean ± SD. The normality of distribution of data was assessed using Shapiro-Wilk test. Data comparisons between two groups were performed using an unpaired t-test. Comparisons among multiple groups were performed using one-way ANOVA, followed by Tukey's multiple-comparisons test. $P<0.05$ was considered to indicate a statistically significant difference.

Results

Correlation between HNSCC and ferroptosis marker genes. The gene expression data and clinical characteristics of 502 HNSCC and 44 normal tissue samples from the TCGA database were included in the present study (Table SIV). The limma package in the R software was used to study the differentially expressed mRNAs. A total of 1,457 genes were significantly upregulated and 715 downregulated (Fig. 1). Enrichment analysis indicated that the DEGs were enriched in 'cell cycle'. Next, 125 ferroptosis genes were downloaded from the FerrDb database, among which nine were validated ferroptosis-related markers (PTGS2, CHAC1, FTH1, SLC40A1, TF, TFRC, GPX4, HSPB1 and NFE2L2). Pearson correlation analysis was conducted to assess the correlations of expressions between each pair of genes of the above 9 ferroptosis marker genes (Fig. 2A) and the PPI network of these genes was further mapped (Fig. 2B). The results indicated that the expression of most of the gene pairs exhibited a statistical correlation (Table SI). The gene annotations and scores are presented in Table SII.

FTH1, TFRC and TF expression in HNSCC. Venn diagram analysis was used and FTH1, TFRC and TF were screened out as common genes expressed in HNSCC and validated ferroptosis markers (Fig. 2C). Subsequently, the expression distributions of these genes in tumor tissues and normal tissues were analyzed and the results indicated that all the three genes were significantly differentially expressed in HNSCC (FTH1, $P=5.5\times10^{-10}$; TFRC, $P=1.3\times10^{-13}$; and TF, $P=2.1\times10^{-17}$; Fig. 2E-G).

FTH1 is an independent prognostic factor in HNSCC. The associations between ferroptosis marker-related DEGs and survival were then analyzed. The log-rank test was used to compare differences in survival between groups with high and low expression of the genes FTH1 [hazard ratio (HR): 1.562, 95%CI: 1.191-2.051, P=0.00129], TFRC (HR: 1.228, 95%CI: 0.94-1.606, P=0.132) and TF (HR: 0.854, 95%CI: 0.653-1.115, P=0.246; Fig. 3A). Time-receiver ROC analysis was used to compare the predictive accuracy for FTH1 [3-year area under the ROC curve (AUC)=0.585, 95%CI: 0.531-0.639], TFRC (3-year AUC=0.525, 95%CI: 0.470-0.480) and TF (3-year AUC=0.514, 95%CI: 0.460-0.569; Fig. 3B).

Based on the formal results, FTH1, TFRC and TF expression was next validated using Oncomine and the Human Protein Atlas database (Fig. 3C). The brown color indicates positive IHC staining. FTH1 expression was then observed in the digestive system heatmap, indicating that it was mainly expressed in squamous epithelial cells and fibroblasts (Fig. 2D). The above results indicated that FTH1 is an independent prognostic factor for HNSCC.

FTH1 protein expression. IHC observation and an IF assay were further performed to determine the localization and FTH1 expression in HNSCC cells. It is generally considered that FTH1 expression is localized to the cytoplasm and membrane (18). The IHC staining result was fully consistent with this (Fig. 4A). An IF assay was then performed for further confirmation and the results complied with IHC, i.e., fluorescence signals were present in the cytoplasm, while no expression was observed in the nucleus (Fig. 4B).

TanIIA downregulates FTH1 expression in FaDu cells. FTH1 expression in FaDu cells was measured by western blot analysis (Fig. 4C). Normal mucosa cells were used as the control group. FTH1 in FaDu cells was significantly overexpressed compared with the control group ($P<0.05$). Different concentrations (0.25, 0.5 and 1 mg/l) of TanIIA were adopted for FaDu cell treatment. The data obtained confirmed that TanIIA at 0.5 mg/l effectively downregulated FTH1 expression in FaDu cells. Furthermore, it is noteworthy that the P-value in the normal mucosa group indicated no significance compared with that of the normal mucosa + TanIIA group. Whether such a result indicated selectivity of TanIIA should be further investigated in depth.

TanIIA effectively reduces FaDu cell survival and invasion. A CCK-8 assay was adopted for detection of cell survival (Fig. 5A-C). TanIIA treatment was performed at concentrations of 0.25, 0.5 and 1.0 mg/l, and the survival rate was measured at 24, 48 and 72 h, respectively, by determining the mean value. The proportion of live cells in the treatment group (48 h: 70.3%; 72 h: 52.29%) decreased significantly ($P<0.05$) as compared with the control group (48 h: 67.83%; 72 h: 54.35%). The effect of TanIIA exhibited a clear dose-effect relationship (Fig. 5D). A Transwell assay was then performed to observe the invasion of FaDu cells (Fig. 5E). As indicated from the results, FaDu cells exhibited a stronger migration and invasion ability than normal hypopharyngeal cells and treatment with TanIIA significantly attenuated the invasion ability of FaDu cells ($P<0.05$; Fig. 5F). Specifically, under treatment with TanIIA (0.5 mg/l) (Fig. 5G), although the invasion ability of HNSCC (mean=146) remained higher than that of the control (mean=119), the difference was not statistically significant ($P=0.0557$), thereby demonstrating that TanIIA treatment effectively inhibited the invasion ability of FaDu cells.

Discussion

The global annual occurrence of head and neck cancers exceeds 0.5 million, out of which 90% are squamous cell carcinoma, HNSCC (19). The development of HNSCC refers to a multi-step process involving multiple signal transduction pathways and complex cross-talk among the pathways. The rapid advancement of microarray technology has significantly boosted gene expression profiling, gene sequencing and convenient diagnosis of diseases due to its high-throughput characteristics and rapid detection ability.

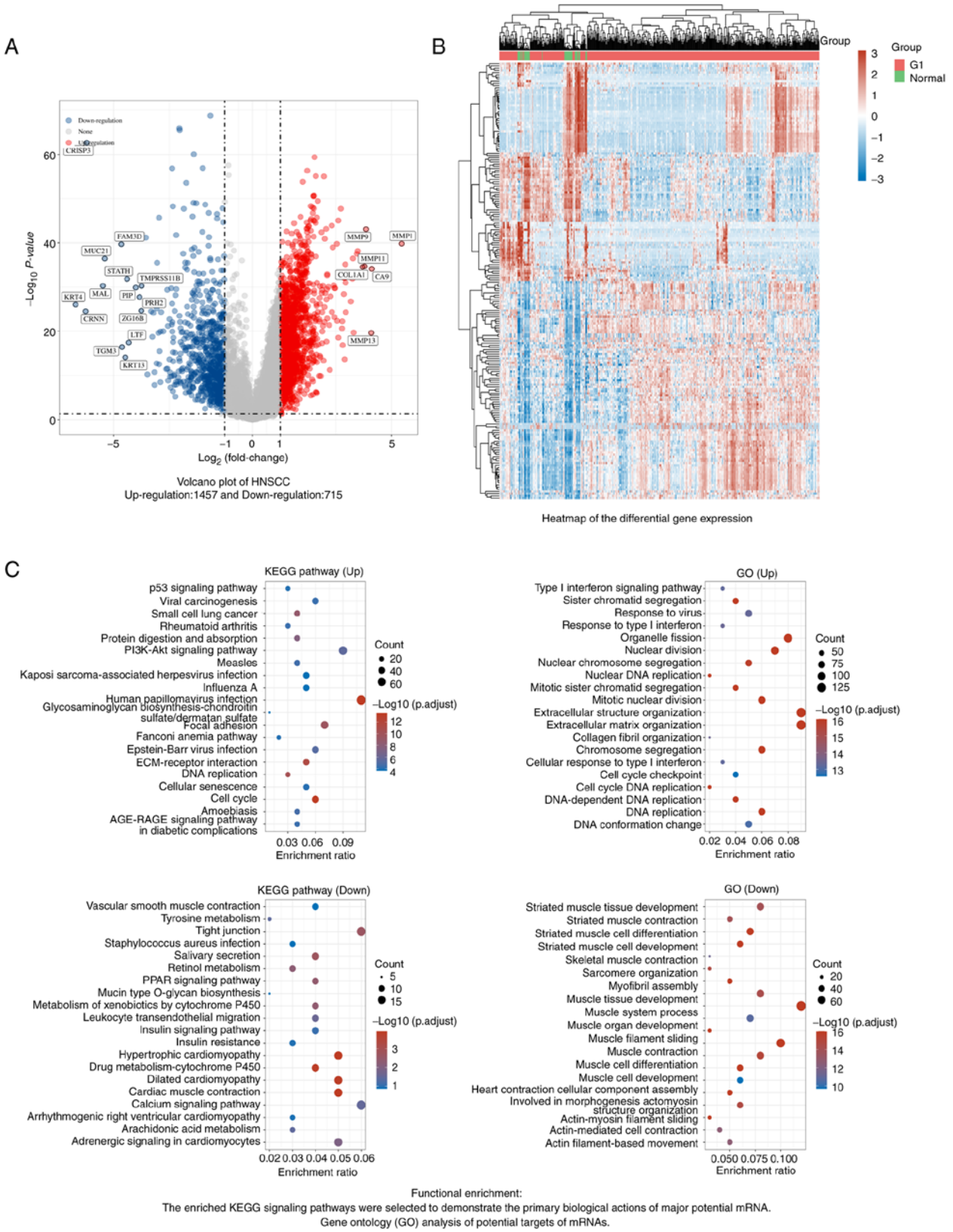

Figure 1. DEGs in HNSCC. (A) Volcano plot: The volcano plot was constructed using the fold change values and adjusted P-value. Red dots indicate upregulated genes (n=1,457) and blue dots indicate downregulated genes (n=715); grey dots indicate genes with insignificant changes. (B) Heatmap of differential gene expression in HNSCC. Different colors represent the trend of gene expression. The top 50 upregulated genes and the top 50 downregulated genes are presented in this figure. (C) Functional enrichment analysis. Left panel: The enriched KEGG signaling pathways were selected to demonstrate the primary biological roles of the differentially expressed mRNAs. The abscissa indicates the gene ratio and the enriched pathways are presented on the ordinate. Right panel: GO analysis of HNSCC DEGs. The biological process, cellular component and molecular function terms of potential targets were clustered using the Cluster Profiler package in R software (v 3.18.0). Colors represent the significance of differential enrichment and the size of the circles represents the number of genes with a larger circle indicating a higher number of genes. Pathways with P<0.05 and false discovery rate <0.05 were considered to be meaningful pathways [enrichment score of-log10(P) >1.3]. HNSCC, head and neck squamous carcinoma; GO, Gene Ontology; KEGG, Kyoto Encyclopedia of Genes and Genomes; Up, upregulated genes; Down, downregulated genes.

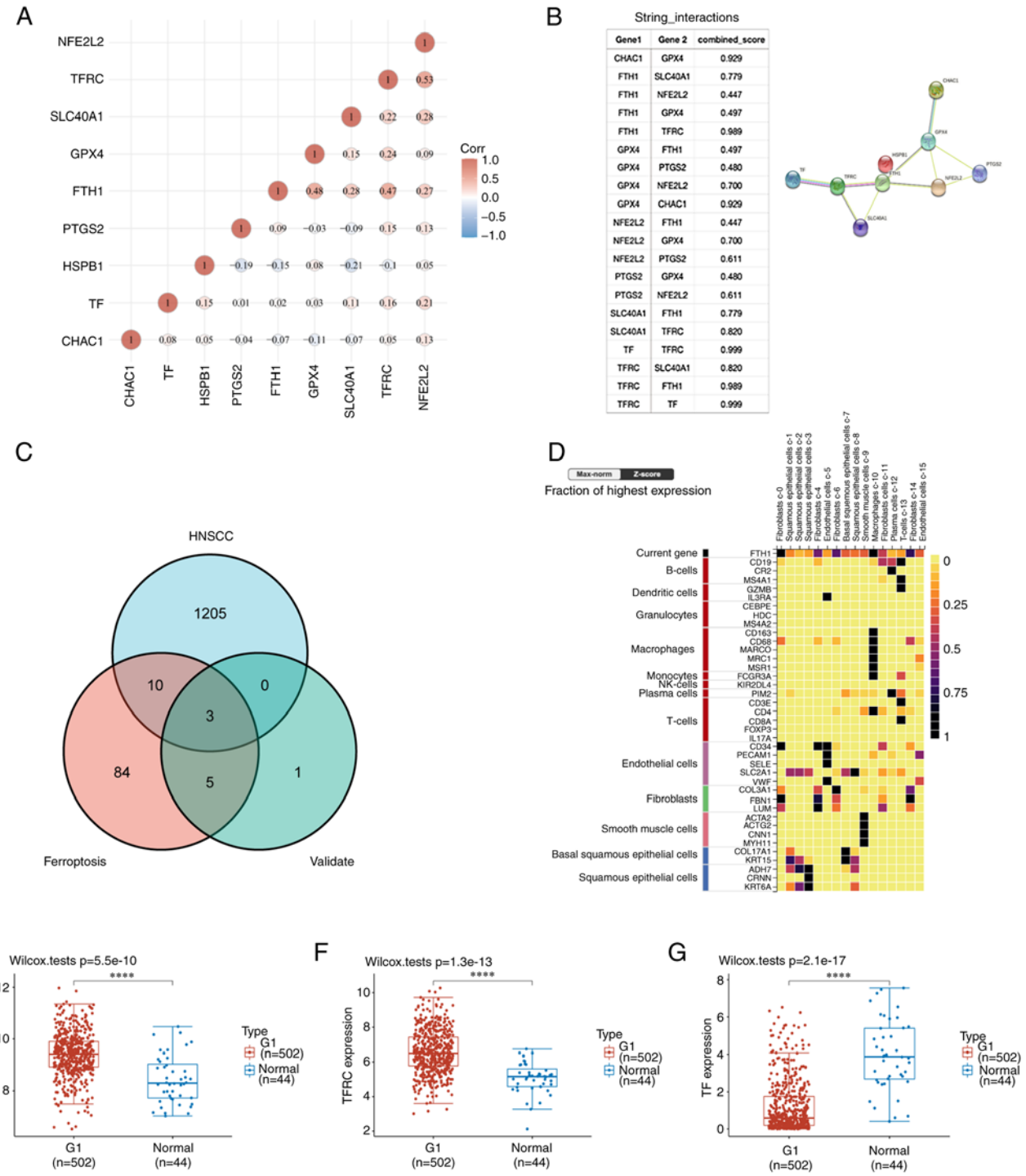

Figure 2. Screened out significantly expressed ferroptosis genes in HNSCC. (A) The correlations among 9 validated ferroptosis genes: A heatmap of the correlation between these 9 genes is provided. The abscissa and ordinate represent genes, different colors represent different correlation coefficients (blue represents a positive correlation whereas red represents a negative correlation), with a darker color indicating a stronger correlation. (B) Annotation of ferroptosis-related differentially expressed marker proteins and their co-expression scores (STRING analysis). (C) Venn diagram of common genes encoding ferroptosis genes that were validated by PCR and are DEGs in HNSCC (R package analysis). (D) Cell type marker heatmap of FTH1 in the alimentary system; FTH1 is mainly expressed in fibroblasts and squamous epithelial cells. Comparison of (E) FTH1, (F) TFRC and (G) TF expression between HNSCC and normal mucosa by the Mann-Whitney U-test (Wilcoxon rank-sum test). Data were acquired from The Cancer Genome Atlas (https://portal.gdc.cancer.gov/) HNSCC database; RNA-seq data in the level 3 HTSeq-FPKM format. ****P<0.0001. HNSCC, head and neck squamous carcinoma; DEG, differentially expressed gene; Corr, correlation coefficient; STRING, Search Tool for the Retrieval of Interacting Genes and Proteins; FTH1, ferritin heavy chain 1; TF, transferrin; TFRC, TF receptor; Seq, sequencing.

Numerous studies have confirmed that ferroptosis has complex roles in tumor progression (20) and regulate the tumor microenvironment (21).

Increasing research studies have confirmed that ferroptosis levels are closely related to HNSCC initiation, progression, recurrence, metastasis and immune escape. Ferroptosis (22) has

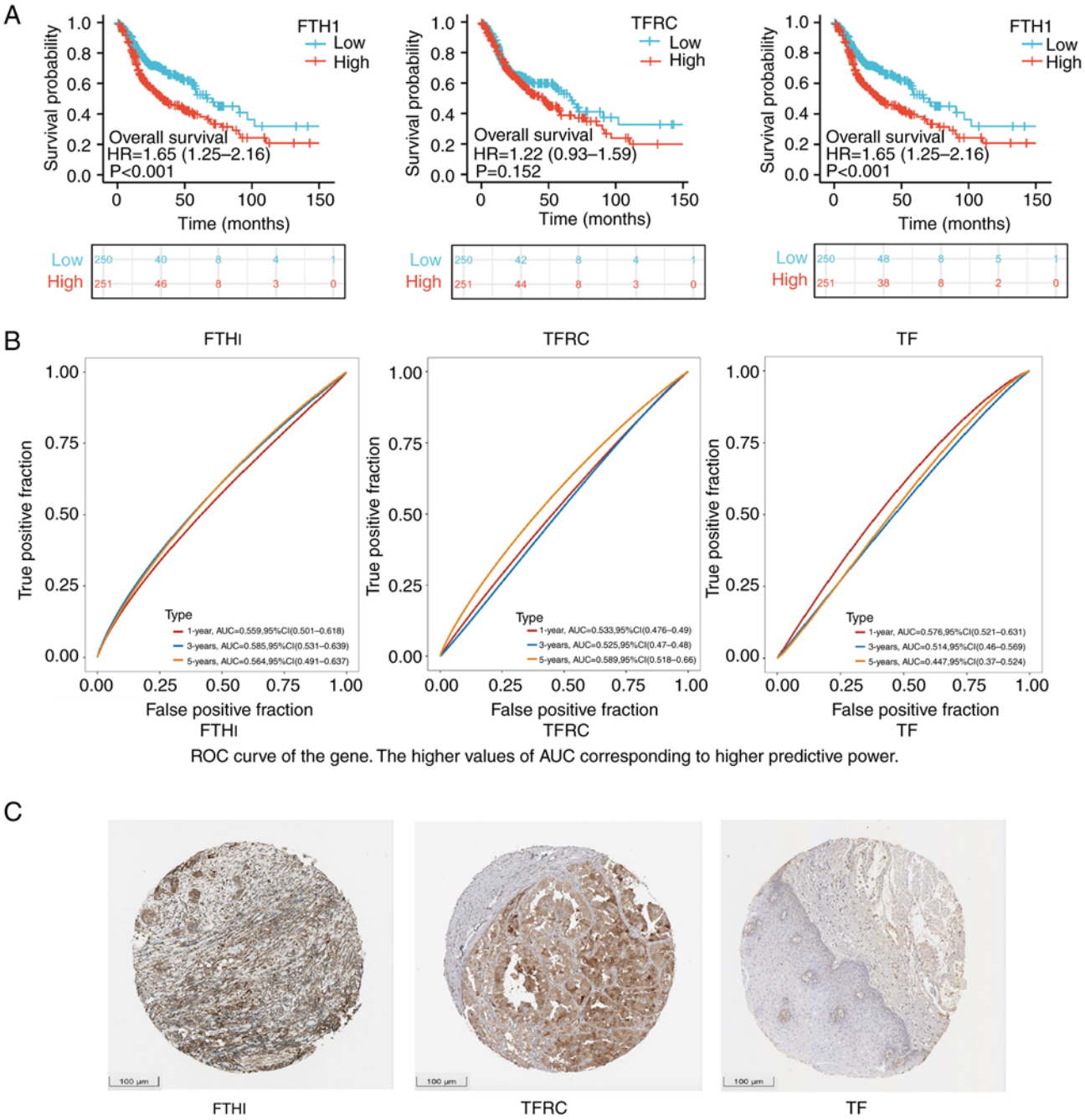

Figure 3. Validated ferroptosis markers and HNSCC. (A) Kaplan-Meier survival analysis of FTH1, TFRC and TF in The Cancer Genome Atlas dataset. Comparison among different groups was performed using the log-rank test. Adjusted HR was computed and 95%CI for HR and median survival time were calculated. (B) ROC curves of FTH1, TFRC and TF at 1,3,5 years. The median values were used as cutoff. A higher AUC corresponds to a higher predictive power. (C) Identification of FTH1, TFRC and TF expression by immunofluorescent staining (scale bar, 100 μm). HNSCC, head and neck squamous carcinoma; HR, hazard ratio (high vs. low expression); FTH1, ferritin heavy chain 1; TF, transferrin; TFRC, TF receptor; AUC, area under the ROC curve; ROC, receiver operating characteristic.

been referred to as the 'new land of cell death'. Distinct from apoptosis, necrosis and autophagy, it refers to an iron-dependent, novel form of programmed cell death with diverse and complex targets involved (e.g., PTGS2, NOX1, FTH1, COX2, GPX4 and ACSl4). A tissue microarray study indicated that patients with high expression of GPX4 had poor survival and the expression of GPX4 has been negatively associated with the immunogenic cell death-related protein calreticulin in an HNSCC tissue array (23). An increasing number of ferroptosis-related targets have been identified as independent prognostic markers for HNSCC (24).

As a widely used TCM compound, TanIIA has already been investigated as a primary or adjuvant therapy with beneficial effects on HNSCC patient survival (10). The latest studies have confirmed that TanIIA increased the level of lipid peroxides and decreased glutathione levels in gastric cancer cells, both of which are markers of ferroptosis (25). Guan *et al* (8) proved that TanIIA caused decreased intracellular glutathione levels and cysteine levels and increased intracellular reactive oxygen species (ROS) levels. Furthermore, p53 knockdown attenuated TanIIA-induced

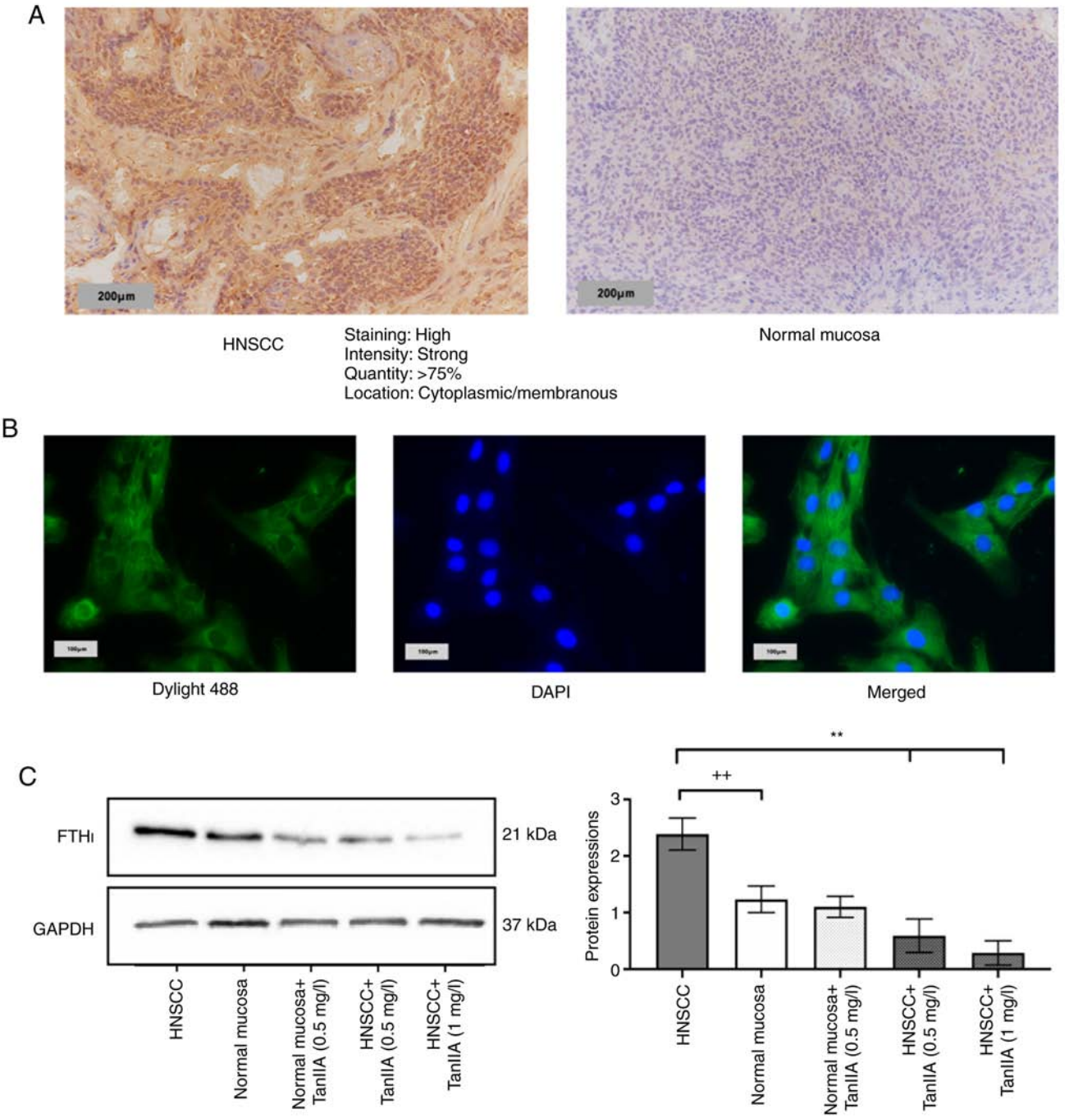

Figure 4. FTH1 expression in FaDu cells and the effects of TanIIA. (A) Immunohistochemistry indicated that FTH1 was mainly expressed in the cytoplasm and cell membrane (scale bars, 200 μm). (B) Immunofluorescence analysis indicated the location of FTH1 expression (scale bars, 100 μm). (C) Western blot analysis was used to investigate FTH1 protein expression levels. Compared to normal mucosa, FTH1 was significantly overexpressed in HNSCC, while TanIIA treatment significantly attenuated FTH1 expression. Experiments were repeated three times and run in triplicate. $^{++}$P<0.01, compared with the control group (Normal mucosa); **P<0.01, compared with the HNSCC group. HNSCC, head and neck squamous carcinoma; FTH1, ferritin heavy chain 1; Tan IIA, Tanshinone IIA.

lipid peroxidation and ferroptosis in a BGC-823 xenograft model. The above studies revealed that TanIIA has significant impacts on cancer cells, partially by inducing ferroptosis. Therefore, it is reasonable to assume that TanIIA may regulate HNSCC progression through ferroptosis-related marker genes.

In the present study, by listing all DEGs in HNSCC and validated marker genes for ferroptosis, three possible targets were screened out: FTH1, TFRC and TF. In a TGCA prognostic analysis, FTH1 was indicated to be an independent prognostic factor of HNSCC.

Iron is an essential element required by cells and has been described as a key player in ferroptosis (26). Ferritin is a protein complex that stores iron in a bioavailable, nontoxic form (27). FTH1 is the main subunit for ferritin's function, which covers a ferroxidase active center responsible for regulating the oxidation and integration of ferric ions. Upstream of the transcription start site of ferritin

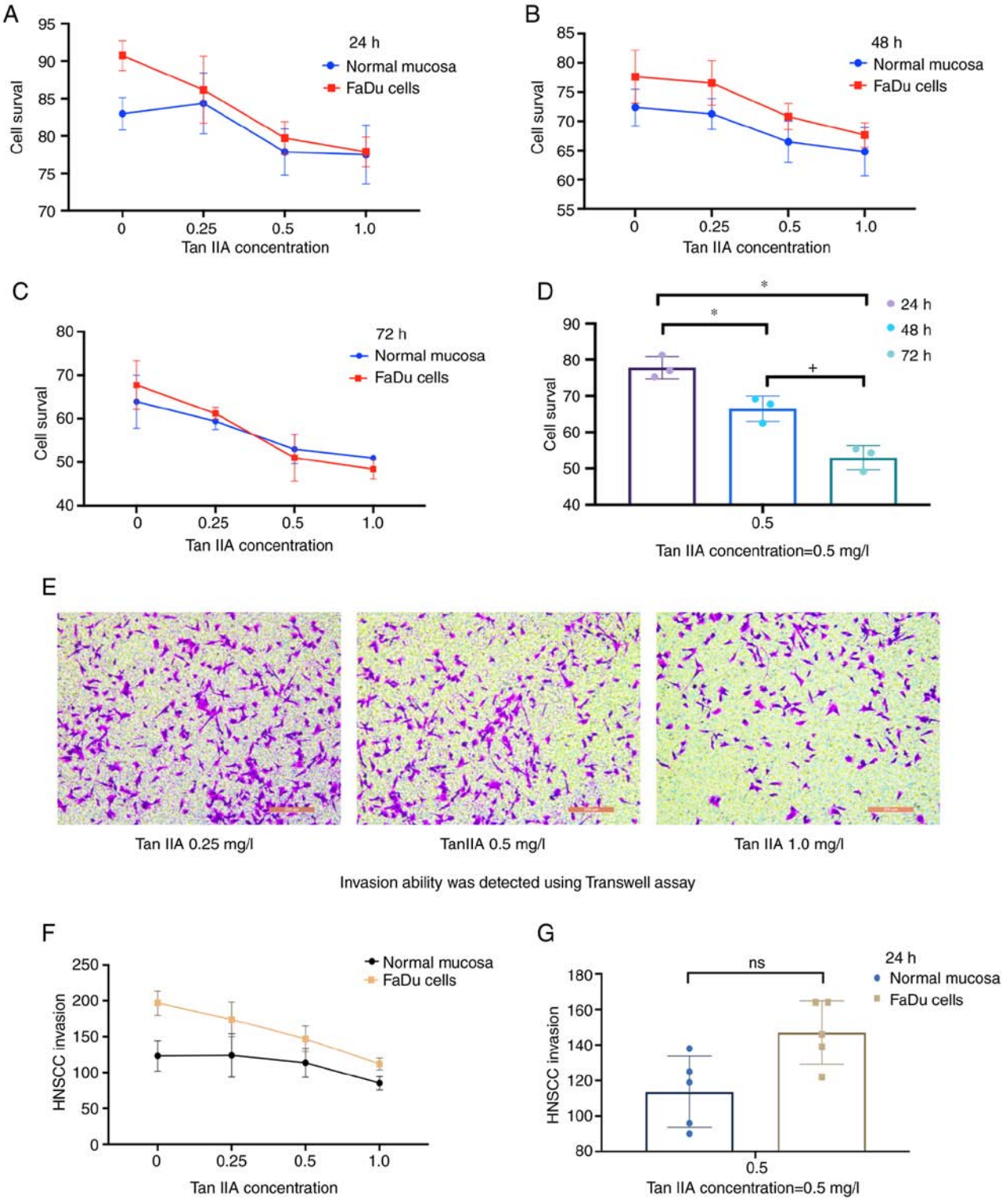

Figure 5. A Cell Counting Kit-8 assay was used to detect the cell survival rate at (A) 24 h, (B) 48 h and (C) 72 h. The blue color represents the control group and the red color represents the FaDu cell group. The survival rate of FaDu cells after TanIIA treatment was lower than that of the control group with a dose-dependent effect. (D) A comparison of each group at a 0.5 mg/l concentration of TanIIA was provided to assess whether the effects were enhanced over time (*P<0.05, compared with 24 h group; +P<0.05, compared with 48 h group). (E) Invasion of FaDu cells in the presence of different concentrations (0.25, 0.5 and 1 mg/l) of TanIIA measured by a Transwell assay (scale bars, 200 μm). (F) Quantitative evaluation of the Transwell assay results indicated that, compared with the control group, FaDu cells exhibited increased invasion ability *in vitro* (*P<0.05), which was attenuated by TanIIA treatment (+P<0.05). (G) Compared with the control group at 0.5 mg/l concentration TanIIA at 24 h. Statistical analysis suggested (P=0.0557) no significant between TanIIA +FaDu cells and Para cancer control, indicating that TanIIA effectively reduced FaDu cells invasion. Tan IIA, Tanshinone IIA; ns, no significance; HNSCC, head and neck squamous carcinoma.

heavy chain contained an antioxidant response element, which could protect cells from oxidative damage, thereby avoiding apoptosis by responding to oxidative reactions (28). This feature makes FTH1 closely related to numerous biological processes such as oxidative stress (29), cell differentiation (30) and neuronal functions (31). Previous work has

shown that FTH1 expression is increased in several human cancers including squamous cell carcinoma, the study by Yang *et al* (32) indicated that long non-protein-coding RNA FTH1 pseudogene 3 was significantly up-regulated in Esophageal squamous cell carcinoma tissues and cells and was critical to the course of tumor formation. Also, the FTH1 expression level is associated with the survival rate of oral squamous cell carcinoma (33). Silencing of FTH1 or reducing its expression has been proved can significantly inhibit carcinogenesis, mainly by promoting cell death (34), inhibiting metastasis (35), and attenuating tumor cell invasion (36). Here we proved that FTH1 is a validated ferroptosis marker gene that significantly impacts HNSCC prognosis, which is mainly expressed in squamous epithelial cells and fibroblasts in the human digestive system.

TanIIA is a pharmacologically active lipophilic component of *Salvia miltiorrhiza* extract, which shares a history of high repute in TCM (37). TanIIA has demonstrated potent tumor inhibitory effects against various types of tumor cell (38); the underlying mechanism involves regulation of the cell cycle (39), suppresses cell proliferation and induces apoptosis (40), inhibits tumor invasion and metastasis, inhibits angiogenesis (41) and reverses tumor multi-drug resistance (42). Xu *et al* (43) demonstrated that TanIIA enhances the antitumor activity of chemotherapeutic drugs and increases the sensitivity of FaDu cells to radiotherapy. Ding *et al* (44) examined the underlying mechanisms and indicated that TanIIA exerted a strong radiosensitizing effect due to enhanced ROS generation and autophagy. Here, CCK-8 and Transwell assays were used to determine the effects of TanIIA on the cell survival and invasion ability in an attempt to examine its pharmacological effects, indicating that at certain concentrations, TanIIA significantly promoted FaDu cell death and attenuated its invasion ability with a dose-effect relationship.

It is generally accepted that FaDu cells exhibit the biological characteristics of high proliferation and invasion (45), which makes treatment of HNSCC relatively difficult. In patients with early-stage HNSCC, surgery and radiotherapy act as the mainstays of treatment, whereas 70-80% of patients are already locally advanced or advanced at the initial presentation. For these patients, the 5-year survival rate was only 40% or even less (46). As reported by a previous study, the median survival time of patients was only 10 months once HNSCC had recurred or metastasized (47). Thus, adjuvant therapies are critical to HNSCC treatment. To date, cisplatin remains the treatment of choice for HNSCC, whereas its development of resistance and toxicity cannot be ignored. Given all the above, finding an effective drug with fewer and less severe side effects is a promising solution. The present study proved that a certain concentration of TanIIA (≥0.5 mg/l) was able to significantly attenuate the protein expression of the prognostic factor FTH1.

In summary, the present study highlights a novel perspective in the clinical treatment of HNSCC and provides a theoretical basis for developing TanIIA for use in co-treatment for HNSCC. By identifying the relationship between ferroptosis markers and HNSCC, a ferroptosis coregulated gene was screened out, which was able to significantly affect HNSCC prognosis. The present study was the first, to the best of our knowledge, to indicate that TanIIA treatment drastically inhibited FTH1 expression in FaDu cells, significantly affected cell survival and suppressed the invasive capacity of FaDu cells. However, the present study had several limitations. FTH1 serves as a vital regulator of ferroptosis, which is generally considered a suppressor of ferroptosis (48), its specific gene function still requires further study using the knockdown or knockout method. The STRING data of the present study indicated that FTH1 is associated with ferroptosis markers including GPX4, SLC40A1, TFRC and NFE2L2, so the downstream signaling pathways are worth further investigating. In addition, as TanIIA is a natural antineoplastic drug, it is also important to perform clinical research on whether dose escalation increases with long-term use and if this would bring side effects.

Acknowledgements

The authors would like to thank Dr Pin Dong (Otolaryngology-Head and Neck Surgery, Shanghai General Hospital, Shanghai, China) for reviewing this article for technical accuracy and for providing valuable suggestions.

Funding

This study was supported by The National Natural Science Foundation of China (grant no. 81800893).

Availability of data and materials

The datasets used and/or analyzed during the current study are available from the corresponding author on reasonable request.

Authors' contributions

WM and BW designed the experiments and drafted the manuscript. WM and JD performed the experiments and analyzed and interpreted the data. YL helped with data collection and analysis. RH coordinated the research and participated in the experimental design. All authors were involved in critically revising the manuscript, and have read and approved the final manuscript. WM and BW confirm the authenticity of all the raw data.

Ethics approval and consent to participate

This work was approved by the Ethics Committee of Shanghai General Hospital (Shanghai, China).

Patient consent for publication

Not applicable.

Competing interests

The authors declare that they have no competing interests.

References

1. Blanchard P, Landais C, Lacas B, Petit C, Bourhis J and Pignon JP: SP-010: Update of the meta-analysis of chemotherapy in head and neck cancer (MACH-NC). Radiother Oncol 122: 9, 2017.

2. Ye J, Jiang X, Dong Z, Hu S and Xiao M: Low-concentration PTX and RSL3 inhibits tumor cell growth synergistically by inducing ferroptosis in mutant p53 hypopharyngeal squamous carcinoma. Cancer Manag Res 11: 9783-9792, 2019.
3. Lee J, Ji HY, Kim MS and Roh JL: Epigenetic reprogramming of epithelial-mesenchymal transition promotes ferroptosis of head and neck cancer. Redox Biol 37: 101697, 2020.
4. Roh JL, Kim EH, Jang H and Shin D: Nrf2 inhibition reverses the resistance of cisplatin-resistant head and neck cancer cells to artesunate-induced ferroptosis. Redox Biol 11: 254-262, 2017.
5. Mou Y, Wang J, Wu J, He D, Zhang C, Duan C and Li B: Ferroptosis, a new form of cell death: Opportunities and challenges in cancer. J Hematol Oncol 12: 34, 2019.
6. Kong N, Chen X, Feng J, Duan T, Liu S, Sun X, Chen P, Pan T, Yan L, Jin T, *et al*: Baicalin induces ferroptosis in bladder cancer cells by downregulating FTH1. Acta Pharm Sin B 11: 4045-4054, 2021.
7. Zhu S, Yu Q, Huo C, Li Y, He L, Ran B, Chen J, Li Y and Liu W: Ferroptosis: A novel mechanism of artemisinin and its derivatives in cancer therapy. Curr Med Chem 28: 329-345, 2021.
8. Guan Z, Chen J, Li X and Dong N: Tanshinone IIA induces ferroptosis in gastric cancer cells through p53-mediated SLC7A11 down-regulation. Biosci Rep 40: BSR20201807, 2020.
9. Qian J, Cao Y, Zhang J, Li L, Wu J, Wei G, Yu J and Huo J: Tanshinone IIA induces autophagy in colon cancer cells through MEK/ERK/mTOR pathway. Transl Cancer Res 9: 6919-6928, 2020.
10. Zhao YX, Luo D, Zhang YH, Shen B, Wang BX and Sun ZF: The effect of tanshinone IIA potentiates the effects of cisplatin in Fadu cells in vitro through downregulation of survivin. Lin Chung Er Bi Yan Hou Tou Jing Wai Ke Za Zhi 31: 781-784, 2017 (In Chinese).
11. He L, Liu YY, Wang K, Li C, Zhang W, Li ZZ, Huang XZ and Xiong Y: Tanshinone IIA protects human coronary artery endothelial cells from ferroptosis by activating the NRF2 pathway. Biochem Biophys Res Commun 575: 1-7, 2021.
12. Zhou N and Bao J: FerrDb: A manually curated resource for regulators and markers of ferroptosis and ferroptosis-disease associations. Database (Oxford) 2020: baaa021, 2020.
13. von Mering C, Huynen M, Jaeggi D, Schmidt S, Bork P and Snel B: STRING: A database of predicted functional associations between proteins. Nucleic Acids Res 31: 258-261, 2003.
14. Shannon P, Markiel A, Ozier O, Baliga NS, Wang JT, Ramage D, Amin N, Schwikowski B and Ideker T: Cytoscape: A software environment for integrated models of biomolecular interaction networks. Genome Res 13: 2498-2504, 2003.
15. Obuchowski NA and Bullen JA: Receiver operating characteristic (ROC) curves: Review of methods with applications in diagnostic medicine. Phys Med Biol 63: 07TR01, 2018.
16. Uhlen M, Oksvold P, Fagerberg L, Lundberg E, Jonasson K, Forsberg M, Zwahlen M, Kampf C, Wester K, Hober S, *et al*: Towards a knowledge-based human protein atlas. Nat Biotechnol 28: 1248-1250, 2010.
17. Xu LP: Studies on the inhibition of AT#9 on three tumour cells proliferation by cell counting-kit 8. Journal of North Pharmacy 9: 43-44, 2012 (In Chinese).
18. Di Sanzo M, Quaresima B, Biamonte F, Palmieri C and Faniello MC: FTH1 pseudogenes in cancer and cell metabolism. Cells 9: 2554, 2020.
19. Liu C, Guo T, Xu G, Sakai A, Ren S, Fukusumi T, Ando M, Sadat S, Saito Y, Khan Z, *et al*: Characterization of alternative splicing events in HPV-negative head and neck squamous cell carcinoma identifies an oncogenic DOCK5 variant. Clin Cancer Res 24: 5123-5132, 2018.
20. Hassannia B, Vandenabeele P and Vanden Berghe T: Targeting ferroptosis to iron out cancer. Cancer Cell 35: 830-849, 2019.
21. Zhang K, Ping L, Du T, Liang G, Huang Y, Li Z, Deng R and Tang J: A ferroptosis-related lncRNAs signature predicts prognosis and immune microenvironment for breast cancer. Front Mol Biosci 8: 678877, 2021.
22. Jiang X, Stockwell BR and Conrad M: Ferroptosis: Mechanisms, biology and role in disease. Nat Rev Mol Cell Biol 22: 266-282, 2021.
23. Zhao YY, Lian JX, Lan Z, Zou KL, Wang WM and Yu GT: Ferroptosis promotes anti-tumor immune response by inducing immunogenic exposure in HNSCC. Oral Dis: Nov 12, 2021 (Epub ahead of print).
24. Tang Y, Li C, Zhang YJ and Wu ZH: Ferroptosis-related long non-coding RNA signature predicts the prognosis of head and neck squamous cell carcinoma. Int J Biol Sci 17: 702-711, 2021.
25. Ni H, Ruan G, Sun C, Yang X, Miao Z, Li J, Chen Y, Qin H, Liu Y, Zhang L, *et al*: Tanshinone IIA inhibits gastric cancer cell stemness through inducing ferroptosis. Environ Toxicol 37: 192-200, 2022.
26. Jiang Y, Mao C, Yang R, Yan B, Shi Y, Liu X, Lai W, Liu Y, Wang X, Xiao D, *et al*: EGLN1/c-Myc induced lymphoid-specific helicase inhibits ferroptosis through lipid metabolic gene expression changes. Theranostics 7: 3293-3305, 2017.
27. Plays M, Müller S and Rodriguez R: Chemistry and biology of ferritin. Metallomics 13: mfab021, 2021.
28. Scaramuzzino L, Lucchino V, Scalise S, Conte ML, Zannino C, Sacco A, Biamonte F, Parrotta EI, Costanzo FS and Cuda G: Dissecting the molecular response of human Escs to iron-mediated oxidative stress by genetic silencing of FTH1 gene. Res Sq 1: 1-28, 2021.
29. Lee JH, Jang H, Cho EJ and Youn HD: Ferritin binds and activates p53 under oxidative stress. Biochem Biophys Res Commun 389: 399-404, 2009.
30. Di Sanzo M, Aversa I, Santamaria G, Gagliardi M, Panebianco M, Biamonte F, Zolea F, Faniello MC, Cuda G and Costanzo F: FTH1P3, a novel H-ferritin pseudogene transcriptionally active, is ubiquitously expressed and regulated during cell differentiation. PLoS One 11: e0151359, 2016.
31. Mu T, Qin Y, Liu B, He X, Liao Y, Sun J, Qiu J, Li X, Zhong Y and Cai J: In vitro neural differentiation of bone marrow mesenchymal stem cells carrying the FTH1 reporter gene and detection with MRI. Biomed Res Int 2018: 1978602, 2018.
32. Yang L, Sun K, Chu J, Qu Y, Zhao X, Yin H, Ming L, Wan J and He F: Long non-coding RNA FTH1P3 regulated metastasis and invasion of esophageal squamous cell carcinoma through SP1/NF-kB pathway. Biomed Pharmacother 106: 1570-1577, 2018.
33. Zhang CZ: Long non-coding RNA FTH1P3 facilitates oral squamous cell carcinoma progression by acting as a molecular sponge of miR-224-5p to modulate fizzled 5 expression. Gene 607: 47-55, 2017.
34. Muhammad JS, Bajbouj K, Shafarin J and Hamad M: Estrogen-induced epigenetic silencing of FTH1 and TFRC genes reduces liver cancer cell growth and survival. Epigenetics 15: 1302-1318, 2020.
35. Li J, Lama R, Galster SL, Inigo JR, Wu J, Chandra D, Chemler SR and Wang X: Small-molecule MMRi62 induces ferroptosis and inhibits metastasis in pancreatic cancer via degradation of ferritin heavy chain and mutant p53. Mol Cancer Ther 21: 535-455, 2022.
36. Huang HX, Yang G, Yang Y, Yan J, Tang XY and Pan Q: TFAP2A is a novel regulator that modulates ferroptosis in gallbladder carcinoma cells via the Nrf2 signalling axis. Eur Rev Med Pharmacol Sci 24: 4745-4755, 2020.
37. Ansari MA, Khan FB, Safdari HA, Almatroudi A, Alzohairy MA, Safdari M, Amirizadeh M, Rehman S, Equbal MJ and Hoque M: Prospective therapeutic potential of Tanshinone IIA: An updated overview. Pharmacol Res 164: 105364, 2021.
38. Zhang Y, Jiang P, Ye M, Kim SH, Jiang C and Lü J: Tanshinones: Sources, pharmacokinetics and anti-cancer activities. Int J Mol Sci 13: 13621-13666, 2012.
39. Che XH, Park EJ, Zhao YZ, Kim WH and Sohn DH: Tanshinone II A induces apoptosis and S phase cell cycle arrest in activated rat hepatic stellate cells. Basic Clin Pharmacol Toxicol 106: 30-37, 2010.
40. Won SH, Lee HJ, Jeong SJ, Lee HJ, Lee EO, Jung DB, Shin JM, Kwon TR, Yun SM, Lee MH, *et al*: Tanshinone IIA induces mitochondria dependent apoptosis in prostate cancer cells in association with an inhibition of phosphoinositide 3-kinase/AKT pathway. Biol Pharm Bull 33: 1828-1834, 2010.
41. Sui H, Zhao J, Zhou L, Wen H, Deng W, Li C, Ji Q, Liu X, Feng Y, Chai N, *et al*: Tanshinone IIA inhibits β-catenin/VEGF-mediated angiogenesis by targeting TGF-β1 in normoxic and HIF-1α in hypoxic microenvironments in human colorectal cancer. Cancer Lett 403: 86-97, 2017.
42. Fan Q, Fan GJ, Yang PM and Zhao JY: Effect of tanshinone microemulsion on reversing MDR in human tumor cells. Zhongguo Zhong Yao Za Zhi 29: 1079-1081, 2004 (In Chinese).
43. Xu H, Hao YL, Xu LN, Chen L and Xu FW: Tanshinone sensitized the antitumor effects of irradiation on laryngeal cancer via JNK pathway. Cancer Med 7: 5187-5193, 2018.
44. Ding L, Wang S, Qu X and Wang J: Tanshinone IIA sensitizes oral squamous cell carcinoma to radiation due to an enhanced autophagy. Environ Toxicol Pharmacol 46: 264-269, 2016.

45. Johnson DE, Burtness B, Leemans CR, Lui VWY, Bauman JE and Grandis JR: Head and neck squamous cell carcinoma. Nat Rev Dis Primers 6: 92, 2020.
46. Ortiz-Cuaran S, Bouaoud J, Karabajakian A, Fayette J and Saintigny P: Precision medicine approaches to overcome resistance to therapy in head and neck cancers. Front Oncol 11: 614332, 2021.
47. Gougis P, Moreau Bachelard C, Kamal M, Gan HK, Borcoman E, Torossian N, Bièche I and Le Tourneau C: Clinical development of molecular targeted therapy in head and neck squamous cell carcinoma. JNCI Cancer Spectr 3: pkz055, 2019.
48. Li X, Si W, Li Z, Tian Y, Liu X, Ye S, Huang Z, Ji Y, Zhao C, Hao X, *et al*: miR-335 promotes ferroptosis by targeting ferritin heavy chain 1 in *in vivo* and *in vitro* models of Parkinson's disease. Int J Mol Med 47: 61, 2021.